ESC European Society of Cardiology

Cardiovascular Research (2018) **114**, 1629–1641
doi:10.1093/cvr/cvy131

Sirtuin 1 activation attenuates cardiac fibrosis in a rodent pressure overload model by modifying Smad2/3 transactivation

Antoinette Bugyei-Twum[1,2], Christopher Ford[1], Robert Civitarese[1], Jessica Seegobin[1], Suzanne L. Advani[1], Jean-Francois Desjardins[1], Golam Kabir[1], Yanling Zhang[1], Melissa Mitchell[1], Jennifer Switzer[1], Kerri Thai[1], Vanessa Shen[1], Armin Abadeh[1], Krishna K. Singh[1], Filio Billia[3], Andrew Advani[1], Richard E. Gilbert[1], and Kim A. Connelly[1,2]*

[1]Division of Cardiology, Keenan Research Centre for Biomedical Science, St. Michael's Hospital, 209 Victoria Street, Toronto, Ontario M5B 1T8, Canada;[2]Institute of Medical Science, University of Toronto, 1 King's College Circle, Toronto, Ontario M5S 1A8, Canada; and [3]Division of Cardiology, Peter Munk Cardiac Centre, Toronto General Hospital, University Health Network, University of Toronto, Toronto, Ontario, Canada

Received 28 February 2018; revised 3 May 2018; editorial decision 7 May 2018; accepted 17 May 2018; online publish-ahead-of-print 25 May 2018

Time for primary review: 15 days

Aims Transforming growth factor β1 (TGF-β1) is a prosclerotic cytokine involved in cardiac remodelling leading to heart failure (HF). Acetylation/de-acetylation of specific lysine residues in Smad2/3 has been shown to regulate TGF-β signalling by altering its transcriptional activity. Recently, the lysine de-acetylase sirtuin 1 (SIRT1) has been shown to have a cardioprotective effect; however, SIRT1 expression and activity are paradoxically reduced in HF. Herein, we investigate whether pharmacological activation of SIRT1 would induce cardioprotection in a pressure overload model and assess the impact of SIRT1 activation on TGF-β signalling and the fibrotic response.

Methods and results Eight weeks old male C57BL/6 mice were randomized to undergo sham surgery or transverse aortic constriction (TAC) to induce pressure overload. Post-surgery, animals were further randomized to receive SRT1720 or vehicle treatment. Echocardiography, pressure–volume loops, and histological analysis revealed an impairment in cardiac function and deleterious left ventricular remodelling in TAC-operated animals that was improved with SRT1720 treatment. Genetic ablation and cell culture studies using a Smad-binding response element revealed SIRT1 to be a specific target of SRT1720 and identified Smad2/3 as a SIRT1 specific substrate.

Conclusion Overall, our data demonstrate that Smad2/3 is a specific SIRT1 target and suggests that pharmacological activation of SIRT1 may be a novel therapeutic strategy to prevent/reverse HF via modifying Smad activity.

Keywords Heart failure • Fibrosis • Hypertrophy • TGF-β signalling • Sirtuin 1

1. Introduction

Despite advances in medical therapy, including neuro-hormonal blockade and the use of cardiac resynchronization therapy, mortality from congestive heart failure (HF) remains unacceptably high, at 25.2% per year.[1] As a result, urgent therapies are required to reduce mortality and morbidity.

A significant body of data has emerged which identifies that overexpression of the pro-fibrotic growth factor transforming growth factor β1 (TGF-β1) leads to cardiac hypertrophy and fibrosis culminating in HF.[2–9] The binding of TGF-β1 to its receptor leads to the nuclear translocation of key TGF-β signalling intermediates, namely Smad2 and Smad3, which increase collagen transcription/fibrosis and mediate cell–cell communication. Regulation of TGF-β signalling is highly complex and can be manipulated at multiple levels with well-described canonical/non-canonical signalling pathways enabling precise regulation.[10] The modification of specific lysine residues by acetylation and de-acetylation has been identified as a major regulator of gene and protein function.[11] Of particular rel-

* Corresponding author. Tel: +1 416 864 5201; fax: +1 416 864 5571, E-mail: connellyk@smh.ca

evance to this study, TGF-β signalling was among the first target to be identified as modifiable by lysine acetylation.[12] Ross *et al.*[13] using an *in vitro* transcription system demonstrated that lysine acetylation/de-acetylation is an absolute requirement for Smad-mediated transcription.

Sirtuins, a family of nicotine adenine di-nucleotide (NAD+) dependent de-acetylating enzymes, were originally identified as key enzymes that modulate life expectancy in yeast, *Caenorhabditis elegans*, *Drosophila*, and mice.[14] There are seven known mammalian sirtuins; however, most research has focused on sirtuin 1 (SIRT1), the ortholog of silent information regulator protein 2 that is responsible for life extension in yeast.[15] Substrates of SIRT1 include proteins that modulate chromatin folding, metabolic regulation, and stress responses. Accordingly, SIRT1 has been repeatedly implicated not only in the ageing process, but also in cancer, cardiovascular disease, and neurodegenerative disorders.[16,17]

Recent data by our group demonstrate that with the development of HF, a reduction in SIRT1 expression occurs. Accordingly, it was thought that enhancing SIRT1 activity through pharmacological manipulation might prevent the development of HF. Recently, a number of novel SIRT1 activators have been developed. Amongst these is SRT1720, a small molecule that dramatically increases SIRT1 de-acetylase activity (greater than seven-fold when compared with existing SIRT1 activators).[18]

Herein, we hypothesize that loss of SIRT1 expression and activity, as seen with HF, results in unopposed and chronic TGF-β signalling activation. Accordingly, restoration of SIRT1 activity through the use of the SIRT1 activator SRT1720 will reduce TGF-β signalling activation, prevent ventricular remodelling, and improve cardiac function in a clinically relevant animal model of cardiac disease.

2. Methods

2.1 Human biopsies

Human studies were conducted in accordance with the ethical standards of the responsible committee on human experimentation (institutional and national) and in accordance with the Helsinki Declaration of 1975, as revised in 2008. Informed written consent was obtained from patients with end-stage HF before the insertion of a left ventricular assist device (LVAD). Eight left ventricular endocardial specimens were obtained, and excised samples were either snap frozen at -80°C, stored in formalin or embedded in optimal cutting temperature compound and stored at -80°C for subsequent analysis. Three commercially available normal adult human left ventricular (LV) lysates, from different donors, were purchased and used as 'healthy' controls (ScienCell Research Laboratories, Carlsbad, CA, USA; Biochain, Newark, CA, USA; Abcam, Cambridge, MA, USA).

2.2 Animal studies—part I

Mice were housed in a vivarium with constant room temperature of 21 ± 1°C on a 12 h light/dark cycle. The mice were fed standard chow preparation and provided water *ad libitum*. All animal studies were approved by the St. Michael's Hospital Animal Care Committee in accordance with the Guide for the Care and Use of Laboratory Animals (NIH Publication No. 85-23, revised in 2011 by the National Research Council). Forty-five mice were randomized into four groups: (i) sham + vehicle ($n = 14$), (ii) transverse aortic constriction (TAC) + vehicle ($n = 15$), (iii) sham + SRT1720 ($n = 6$), and (iv) TAC + SRT1720 ($n = 10$). All mice randomized to the SRT1720-treated arms of the study received 100 mg/kg of body weight of the compound via gavage once daily for the duration of the study. These mice were also pre-treated with SRT1720 for 1 week prior to TAC or sham surgeries to allow the drug to reach steady-state levels. This approach was taken with the rationale that SRT1720, similar to sirtuin-activating compounds that are safe and found in food, could be used as a prophylactic for hypertensive individuals, with patients taking SRT1720 and anti-hypertensive therapy well before the advent of an adverse event such as an acute myocardial infarction/LV remodelling. All mice were euthanized at 6 weeks post-surgery, following cardiac catheterization. Post-mortem morphometric data were obtained, including detailed heart weights. Cardiac tissue was collected from the apex of the heart and frozen with liquid nitrogen for RNA and protein analyses.

2.3 Transverse aortic constriction

Constriction of the transverse aorta was performed on 8- to 10-week-old mice as previously described.[19] Mice were anaesthetized with 2% isoflurane, intubated, and placed on a respirator. Ventilation rate was adjusted based on body weight of the animal. Body temperature was maintained at 37 ± 1°C by placing the mouse on a heating pad connected to a circulating warm water pump. Midline sternotomy was performed, the aorta was visualized, and a 6.0 Prolene suture was placed around the aorta distal to the brachiocephalic artery. The suture was tightened around a blunt 25- to 26-gauge needle placed adjacent to the aorta. Needle size was selected based on the weight of the mice at time of surgery (20–24 g, 26-gauge needle; 25–30 g, 25-gauge needle) as recommended to induce a 0.4 mm diameter constriction. The needle was removed inducing a narrowing of the transverse aorta. The chest and underlying skin were then closed, and animals were recovered on a respirator. Sham animals underwent a similar procedure with midline sternotomy and aorta visualization without tightening of the suture around the aorta. Both TAC and sham mice received 48 h of pain management via subcutaneous Anafen (5 mg/kg, twice daily) and buprenorphine (0.2 mg/kg, twice daily) injections.

2.4 Animal studies—part II

Male homozygous $SIRT^{Y/Y}$ mice, 8–10 weeks of age, were a kind gift from Michael McBurney, Ottawa, Canada.[20] Twenty mice were housed in a vivarium with constant room temperature of 21 ± 1°C on a 12 h light/dark cycle. The mice were fed standard chow preparation and provided water *ad libitum*. Mice were randomized into two groups: (i) TAC + vehicle ($n = 10$) and (ii) TAC + SRT1720 ($n = 10$). Mice were euthanized 6 weeks post-TAC, following cardiac catheterization.

2.5 Echocardiography

Echocardiography was performed under anaesthetic (1–1.5% isofluorane, 2 L/min oxygen flow rate) and intubation. Echocardiography was performed 48 h post-TAC surgery to confirm successful aortic banding or sham procedure. Mice were then imaged at the 4 week time point to confirm progression or lack of left ventricular hypertrophy. Imaging was also performed at 6 weeks, just prior to end study for final assessment. All echocardiographic assessments were performed using the Vevo® 2100 system and a MS-400 Red probe as previously reported.[21] Novel echocardiographic techniques to assess regional cardiac function such as strain imaging were performed using velocity vector imaging as previously reported.[22,23]

2.6 Cardiac catheterization

Left ventricular cardiac catheterization was performed at end-study under anaesthetic (1–2% isofluorane, 2 L/min oxygen flow rate) with mice intubated. The right internal carotid artery was used for insertion of the catheter and advanced to the aorta, then entered into the left ventricle. Using the pressure conductance data, functional parameters were then calculated with Millar analysis software as previously reported.[21] All animals were euthanized following cardiac catheterization, while under anaesthesia, via cervical dislocation.

2.7 Histopathology

Left ventricular cross-sectional samples were cut and fixed in 10% formalin. Paraffin blocks were cut into 4 μm sections and mounted on charged microscope slides, then left to dry at 35°C for 24–48 h. The extent of cardiac myocyte hypertrophy was determined on haematoxylin and eosin-stained sections, as adapted from a previous study. Approximately 10–20 images were captured at 400× magnification across the sub-endocardium. Circular-shaped cardiac myocytes with nuclei in the sub-endocardium were selected, and the transverse diameter was measured using AxioVision software (Version 4.8.2). The pixel measurement was then converted into μm^2 utilizing known conversions, as previously demonstrated.[24] For each animal, the average diameter of 30–50 cardiac myocytes was calculated. Analysis was conducted in a blinded fashion.

The extent of fibrosis was quantified on picrosirius red (PSR) stained sections. Ten images per animal were captured at 400× magnification from each region of the sub-endocardium. Using ImageScope software, the red colour of the PSR stain was selected from a colour range so that the software may identify it accurately. Calculation of the proportional area stained per image was then determined utilizing ImageScope, and an average was calculated from the 10 representative images per animal, as a percentage of stain as previously reported.[4]

2.8 RNA quantification

Total RNA was isolated from homogenized cardiac apex tissue using TRIzol reagent. Total RNA (2 μg) was converted to cDNA (for a 20 μL reaction) using the High Capacity cDNA Reverse Transcription Kit and stored at -20°C until further analysis.

Measurement of the foetal gene programme was expressed relative to *Rpl13a*, and measurement of Smad2/3 responsive genes were expressed relative to *RPL32A* using MicroAmp® Optical 384-Well Reaction Plates with a ViiA™ 7 Real-Time polymerase chain reaction system, as previously reported.[25] Experiments were performed in triplicates, and data analysis was performed using Applied Biosystems Comparative C_T method. All primer sequences are listed in Supplementary material online, *Table S1*.

2.9 Luciferase reporter assay

Smad-dependent transcriptional activity was assessed by a Smad2/3-responsive reporter construct containing four consecutive Smad-binding elements driving the expression of firefly luciferase (SBE4-Luc). Briefly, human embryonic kidney (HEK) cells were plated (0.15×10^6 cells/well) onto fibronectin-coated plates and after 24 h were co-transfected with 0.4 μg/well SBE4-Luc and 0.2 μg/well of the normalizing vector RL-TK Renilla luciferase. After 16 h, cells were serum starved for 3 h, then incubated with TGF-β1 (2 ng/mL) with and without SRT1720 for 24 h. Cells were then lysed, and luciferase activity was determined using the Dual Luciferase Reporter Assay System kit (Promega) and a luminometer (Lumat 9507; Berthold) according to the manufacturers' instructions. For each condition, treatments were performed in triplicates, and experiments were repeated at least three times. For each sample, firefly luciferase activity was normalized to the Renilla luciferase activity of the same sample. Results were then expressed as fold changes compared with the mean firefly/Renilla ratio of untreated controls.

2.10 Immunoblot and immunofluorescence

Total protein was extracted with ice-cold radioimmunoprecipitation buffer containing a protease inhibitor mixture and quantified with a Bio-Rad Protein Assay Reagent. Protein samples were then separated by SDS-PAGE and transferred onto nitrocellulose membranes. Membranes were blocked with 5% skim milk in TBS-T and probed with the following antibodies from Cell Signaling Technologies, Beverly, MA, USA (GAPDH, 2118; phospho-Smad2, 3101; phospho-Smad3, 9520; phospho-Smad2/3, 8828; Smad3, 9513; Smad2/3, 3102; acetylH3K9/14, 9677; SIRT1 (human), 9475; SIRT1, 2028 (mouse); acetylated-lysine, 9441). Anti-rabbit (7074) or anti-mouse (7076) secondary antibody conjugated to horseradish peroxidase (Cell Signaling Technologies) was subsequently used, and signal was visualized with an enhanced chemiluminescence detection system (Amersham Biosciences). Immunofluorescence signal for phospho-Smad2/3 was visualized using standard immunostaining protocol. Images were captured using a Zeiss LSM700 confocal microscopy and processed using a ZEN imaging software.

2.11 SIRT1 activity assay

Left ventricular tissue samples were cut into small pieces and added to 1 mL of phosphate-buffered saline. Samples were then homogenized using an ultrasonic homogenizer (Model 3000; Biologics Inc.), followed by centrifugation at 500×*g* for 3 min to remove the supernatant. Nuclear and cytoplasmic fractions were prepared using a nuclear/cytosol fractionation kit (BioVision Inc., Mountain View, CA, USA) according to the manufacturer's instructions, and protein concentration for each sub-cellular fraction was determined using the Bradford method (Bio-Rad Laboratories Inc., Hercules, CA, USA). SIRT1 activity was measured using 20 μg of protein from the total nuclear fraction with the aid of a fluorometric SIRT1 activity assay kit (Abcam Inc., Cambridge, MA, USA). Assay was performed according to the manufacturer's instructions, and fluorescence intensity was measured at 3 min intervals for up to 60 min, with excitation at 355 nm and emission at 460 nm.

2.12 Cell culture

Human cardiac fibroblast cells (ScienCell Research Laboratories, Carlsbad, CA, USA) were stimulated with 5 ng/mL TGF-β1 (R&D Biosystems, Minneapolis, MN, USA) in the presence or absence of SRT1720 (5 μmol/L) for 1 h to assess canonical TGF-β activation or 24 h to assess to the expression of TGF-β responsive genes.

2.13 Acetylation assay

HEK cells were seeded to ~80% confluence and transfected with a Smad3 construct (pCMV5B/Flag-Smad3) along with an empty vector or a dominant negative SIRT1 construct (Flag-SIRT1, H355A; Addgene, Cambridge, MA, USA) using Lipofectamine 3000 (Life Technologies, Carslbad, CA, USA) according to the manufacturer's instructions. After 24 h, cells were stimulated with TGF-β1 (5 ng/mL) in the presence or absence of SRT1720 (5 μmol/L) for 24 h. Cells were then fractionated into nuclear and cytoplasmic fractions using a Nuclear/Cytosol Fractionation kit (BioVision, Mountain View, CA, USA). Nuclear fraction (200 μg) was

used, along with a Smad3-specific antibody (Smad3; Cell Signaling Technologies) to immunoprecipitate Smad3. This was followed by immunoblotting with a pan-specific anti-acetylated lysine antibody (Cell Signaling Technologies).

2.14 [^{3}H]-proline incorporation assay

Following serum starvation, primary neonatal rat cardiac fibroblasts were stimulated with 10 ng/mL of TGF-β (R & D Biosystems, Minneapolis, MN, USA) and incubated with [^{3}H]-proline (1 μCi/well, Amersham Biosciences) in the presence or absence of SRT1720 (5 μmol/L) for 44 h. Incorporation of [^{3}H]-proline was measured using a liquid scintillation counter (LS 6000; Beckman Instruments, Beckman Coulter, Mississauga, Canada), as previously reported.

2.15 Statistics

Data are expressed as mean ± standard error of mean (SEM). Statistical significance was determined by two-way ANOVA with Tukey *post hoc* multiple comparison. Student's *t*-test was used when the means of two groups were compared. All statistics were performed using GraphPad Prism 6 (GraphPad Software Inc., San Diego, CA, USA). A *P*-value of <0.05 was considered to indicate statistically significance.

3. Results

3.1 SIRT1 expression is reduced in end-stage human HF

Human left ventricular (LV) biopsy specimens obtained from patients with end-stage coronary artery disease were analysed for SIRT1 expression by western blotting (*Figure 1A*). Total SIRT1 levels were lower in LV samples from patients with end-stage HF when compared with controls. To confirm this observation, an experimental model of HF—a pressure overload model—was used to evaluate the expression of SIRT1 in the LV. Similar to end-stage human HF, SIRT1 expression was also reduced in animals that had underwent TAC (*Figure 1B*).

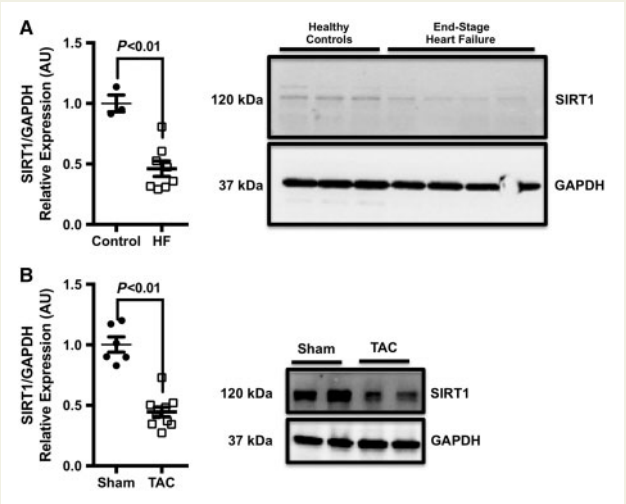

Figure 1 SIRT1 expression is reduced in human end-stage HF and in a murine pressure overload model. (*A*) Representative image of SIRT1 protein expression in end-stage heart failure. Robust SIRT1 expression was noted in healthy controls ($n = 3$) and a significant reduction of SIRT1 protein in LV specimens of patients undergoing LVAD implantation ($n = 8$). (*B*) Similarly, SIRT1 expression was markedly reduced in pressure overload animals ($n = 10$) compared with sham controls ($n = 6$). All data are presented as mean ± SEM; comparison between groups assessed using a two-tailed, unpaired Student's *t*-test.

3.2 SIRT1720 improves cardiac function in pressure overload mice

SRT1720 has previously been reported to extend lifespan and improve cardiac health. However, despite its reported benefits, the molecular mechanisms underlying its protective effects are not completely understood. To investigate the direct effect of pharmacological activation of SIRT1 on the heart, a murine TAC model was used. At 6 weeks post-surgery, TAC-operated animals showed signs of cardiac hypertrophy and pulmonary congestion (*Table 1*). Treatment of TAC-operated animals with SRT1720 significantly reduced LV mass—when indexed to tibia length—without having a pronounced effect on lung weight (*Table 1*).

3.3 SIRT1720 improves aberrant changes in the LV following pressure overload

Echocardiographic assessment of cardiac structure post-pressure overload revealed an increase in LV mass, wall thickness, and the occurrence of LV systolic dysfunction in TAC-operated animals (*Table 2*). These changes were reversed in TAC-operated animals treated with SRT1720 (*Table 2*).

To assess regional cardiac function and to account for changes in loading conditions, vector imaging was employed. TAC-operated animals exhibited impaired radial and longitudinal strain, which was normalized in TAC-operated animals treated with SRT1720 (*Figure 2A–D*). No notable differences were observed between sham-operated animals and those treated with the compound SRT1720.

Pressure–volume loops were used to assess loading insensitive measures of cardiac contractility and relaxation. Steady-state pressure–volume loops revealed worse function in TAC-operated animals when compared with sham-operated controls—with a rightwards and upwards shift of the PV loop (*Figure 3A* and *B*). This was associated with a significant increase in end-systolic pressure (*Figure 3E*). Pre-treatment of TAC-operated animals with SRT1720 resulted in a shift of the steady-state PV loop to the left, indicating an improvement in systolic function (*Figure 3C* and *D*). No change in end-systolic pressure was observed with SRT1720-treatment in shams (*Figure 3E*).

Furthermore, assessment of cardiac contractility using the preload recruitable stroke work index demonstrated a significant increase in TAC-operated animals treated with SRT1720 when compared with vehicle-treated animals (*Figure 3F*). Surprisingly, neither pressure overload nor SRT1720 affected diastolic function, as assessed by end-diastolic pressure, Tau or the slope of the end-diastolic pressure–volume relationship (*Table 3*).

3.4 SRT1720 attenuates pressure overload-induced fibrosis and hypertrophy

Pressure overload resulted in LV fibrosis in TAC-operated animals, as assessed by PSR staining. The amount of PSR staining was significantly reduced in SRT1720-treated TAC-operated animals when compared with vehicle-treated TAC-operated mice (*Figure 4A* and *B*). We also assessed the impact of pressure overload on cardiomyocyte hypertrophy. TAC-operated animals had a larger mean cell size—a 32% increase (272 μm^2 vs. 206 μm^2, $P < 0.0001$) than sham-operated controls (*Figure 4C* and *D*). With SRT1720 treatment, the mean cell size of TAC-operated animals

Table 1 Characteristics of animals

	Sham ($n = 14$)	Sham + SRT1720 ($n = 6$)	TAC ($n = 13$)	TAC + SRT1720 ($n = 9$)
Body weight (g)	29.0 ± 2.6	24.7 ± 1.2*	28.7 ± 2.0	25.7 ± 2.1***
Tibia length (mm)	15.1 ± 0.5	15.8 ± 0.2	16.2 ± 0.6	16.2 ± 0.2
Heart weight (mg)	122.6 ± 2.7	108.5 ± 5.0	180.7 ± 10.6*	146.1 ± 8.1**
HW:BW (mg/g)	4.2 ± 0.1	4.4 ± 0.2	6.3 ± 0.4*	5.7 ± 0.2*
HW:TL (mg/mm)	8.2 ± 0.4	6.9 ± 0.4	11.3 ± 0.9*	9.0 ± 0.5**
LV mass (mg)	86.79 ± 2.0	76.5 ± 3.3	135.6 ± 7.0*	105.6 ± 6.3**
LV:BW (mg/g)	3.0 ± 0.1	3.1 ± 0.2	4.7 ± 0.3*	4.1 ± 0.2*
LV:TL (mg/mm)	5.8 ± 0.3	4.8 ± 0.2	8.5 ± 0.6*	6.5 ± 0.4**
Lung weight (mg)	128.1 ± 3.8	138.2 ± 9.5*	158.2 ± 11.7*	141.7 ± 5.4**
LW:BW (mg/g)	4.4 ± 0.2	5.6 ± 0.4	5.5 ± 0.4	5.6 ± 0.3
LW:TL (g/mm)	8.6 ± 0.3	8.8 ± 0.7	10.0 ± 1.0	8.7 ± 0.3

Data are presented as mean ± SEM.
BW, body weight; HW, heart weight; LW, lung weight; TAC, transverse aortic constriction; TL, tibial length.
*$P < 0.05$ compared with sham using a two-way ANOVA with Tukey's *post hoc* test.
**$P < 0.05$ compared with TAC using a two-way ANOVA with Tukey's *post hoc* test.

Table 2 Echocardiographic data

	Sham ($n = 14$)	Sham + SRT1720 ($n = 6$)	TAC ($n = 11$)	TAC + SRT1720 ($n = 8$)
Cardiac output (mL/min)	18.7 ± 1.3	17.3 ± 1.8	20.4 ± 1.9	19.1 ± 1.2
Ejection fraction (%)	65.3 ± 3.4	70.5 ± 3.4	53.4 ± 4.5*	65.3 ± 2.7**
Fractional area change (%)	54.3 ± 3.0	63.1 ± 4.5	40.9 ± 4.2*	53.6 ± 3.3**
Fractional shortening (%)	36.3 ± 2.5	39.6 ± 2.8	28.0 ± 2.8	35.4 ± 1.9
LVAWD; d (mm)	0.88 ± 0.03	0.86 ± 0.05	1.18 ± 0.05*	1.00 ± 0.05**
LVPWD; d (mm)	0.84 ± 0.04	0.89 ± 0.03	1.14 ± 0.05*	0.98 ± 0.04**
LV mass corr (mg)	105.8 ± 3.1	83.75 ± 5.6	176.3 ± 17.3*	115.3 ± 9.4**

Data are presented as mean ± SEM.
LV mass corr, corrected left ventricular mass; LVAWD; d, left ventricular anterior wall diameter; LVPWD; d, left ventricular posterior wall diameter; TAC, transverse aortic constriction.
*$P < 0.05$ compared with sham using a two-way ANOVA with Tukey's *post hoc* test.
**$P < 0.05$ compared with TAC using a two-way ANOVA with Tukey's *post hoc* test.

was reduced compared with their untreated counterparts (207 μm^2 vs. 272 μm^2, $P < 0.0001$; *Figure 4C* and *D*).

Further analysis of LV tissue revealed the induction of the foetal gene programme in TAC-operated animals (*Table 4*). A decrease in β:α-myosin heavy chain (MHC) ratio (0.89 vs. 3.69, $P < 0.0001$), atrial natriuretic peptide (ANP, 0.51 vs. 3.95; $P < 0.01$), and skeletal alpha-actin expression (SKA, 0.75 vs. 2.63; $P < 0.01$) was observed with SRT1720 treatment, but no significant effect on α-MHC or SERCA2a expression was noted. SRT1720-treated sham-operated animals showed changes in the expression of all foetal genes when compared with untreated sham-operated controls; with α-MHC, β-MHC, and SERCA2a being significant reduced ($P < 0.05$). These changes, however, did not translate to functional or structural changes in the heart as assessed by echocardiography and *in vivo* cardiac catheterization.

3.5 SIRT1 activity is crucial for SRT1720-induced cardioprotection

To investigate the mechanism by which SRT1720 confers cardioprotection, we assessed SIRT1 expression and de-acetylase activity in our TAC model. TAC-operated animals demonstrated a reduction in SIRT1 mRNA expression when compared with sham-operated controls. Treatment with SRT1720 did not alter SIRT1 mRNA expression in either shams or TAC-operated animals (*Figure 5A*). SIRT1 de-acetylase activity was notably reduced (12% reduction c/w sham, $P < 0.05$) in TAC-operated animals when compared with sham-operated controls; however, this was restored with SRT1720 treatment (*Figure 5B*).

To address potential concerns regarding SRT1720's specificity towards SIRT1, a SIRT1 catalytically inactive mouse model was used. In this model, a point mutation at H355Y renders SIRT1 catalytically inactive ($SIRT1^{Y/Y}$); thus the model expresses normal SIRT1 protein but undetectable SIRT1 de-acetylase activity. $SIRT1^{Y/Y}$ displays a similar phenotype to that of SIRT1-null animals. To assess whether the cardioprotective effect of SRT1720 in our pressure overload model is specific to SIRT1 activation, $SIRT1^{Y/Y}$ animals underwent TAC surgery followed by randomization into two groups—vehicle-treated group vs. SRT1720-treated group. No significant differences were noted between SRT1720-treated $SIRT1^{Y/Y}$ animals and the vehicle-treated animals.

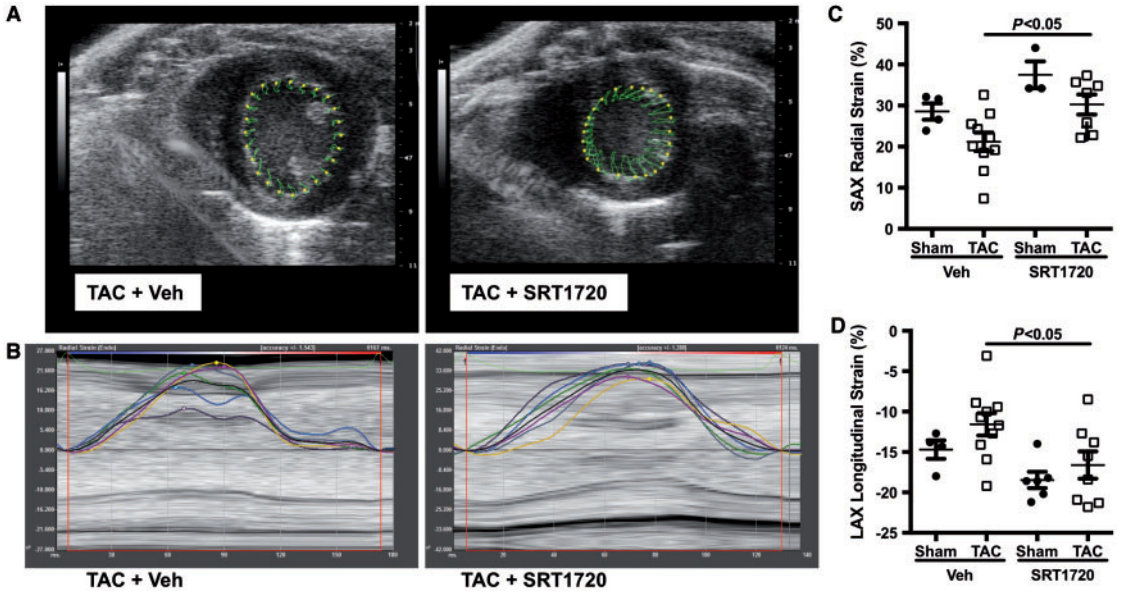

Figure 2 Impaired radial and longitudinal strain in pressure overload mice. Velocity vector imaging was used to assess regional cardiac function in TAC and TAC + SRT1720-treated mice. (*A*) TAC impaired both radial and (*B*) longitudinal strain, which were normalized with SRT1720 treatment. Quantitative data of (*C*) radial (n = 3–10 animals per group) and (*D*) longitudinal strain (n = 4–10 animals per group) are presented as mean ± SEM and analysed using a two-way ANOVA with Tukey's *post hoc* test.

Parameters used to evaluate cardiac function, including LV weight and LV wall thickness, were not altered with SRT1720 treatment (*Figure 5C–E*). Similarly, there were no changes to systolic or diastolic function in the SRT1720-treated SIRT1$^{Y/Y}$ animals. Collectively, these observations suggest that the cardioprotective effect of SRT1720 in our TAC model is contingent on its ability to alter the enzymatic activity of SIRT1.

3.6 SIRT1720 modifies TGF-β signalling and histone H3 acetylation status in the murine heart

TGF-β is a pleiotropic cytokine that has been reported to play a central role in maladaptive changes in response to sustained pressure overload.[6] LV samples from TAC-operated animals and SIRT1720-treated animals were assessed for TGF-β activation. As expected, an increase in Smad2 phosphorylation was observed in TAC-operated animals; this, however, was reduced with SRT1720 treatment (*Figure 6A* and *C*). *In vitro* assessment of the effect of SRT1720 on TGF-β signing also provided similar results. Treatment of human cardiac fibroblast cells with TGF-β1 increased the phosphorylation levels of Smad3, which was reduced with SRT1720 treatment (*Figure 6D*). A reduction of nuclear phospho-Smad2/3 levels with SRT1720 treatment, as assessed by immunofluorescence microscopy, was also noted (*Figure 6E*). As an aside, the acetylation status of histone H3 at lysine residues 9 and 14 was also assessed to gage the enzymatic/de-acetylase activity of SIRT1. The acetylation level of histone H3K9/K14 was elevated in TAC-operated animals and reduced in SRT1720-treated animals (*Figure 6B* and *C*).

To determine whether the effect of SRT1720 on TGF-β signalling was mediated by pharmacological activation of SIRT1 with SRT1720, HEK cells were transfected with a SIRT1 catalytically inactive dominant negative mutant (H355A) and stimulated with TGF-β1, SRT1720, or a combination of the two. Under normal conditions (untransfected HEK cell; without H355A), HEK stimulated with TGF-β1 showed an increase in Smad3 acetylation. This, however, was reduced when cells were pre-treated with SRT1720 prior to TGF-β1 stimulation (*Figure 7A*). In the presence of the H355A SIRT1 dominant negative mutant, SRT1720 was no longer able to reduce Smad3 acetylation levels (*Figure 7A*), suggesting that the presence of a functional SIRT1 protein is required for the SRT1720-mediated decrease of Smad3 acetylation previously observed.

Next, we assessed whether SIRT1720 can alter the transcriptional activity of key intracellular signalling molecules involved in TGF-β signalling—namely Smad2/3. Using a Smad2/3-responsive reporter construct, HEK cells were transfected with a reporter construct containing four consecutive Smad-binding elements driving the expression of firefly luciferase (SBE4-Luc) prior to being stimulated with TGF-β1. Upon stimulation with TGF-β1, Smad2/3 promoter construct activity was robustly enhanced, as assessed by luciferase activity (*Figure 7B*). This, however, was reduced when cells were co-treated with the compound SRT1720 (*Figure 7B*).

To determine the effect of SRT1720 on downstream Smad2/3 activity—specifically, its effect on TGF-induced fibrotic response—^{3}H-proline incorporation was assessed as a measure of collagen synthesis using primary neonatal rat cardiac fibroblast cells and the expression of Smad2/3 responsive genes was assessed using human cardiac fibroblast cells. As anticipated, TGF-β1 increased ^{3}H-proline incorporation (*Figure 7C*) and the expression of Smad2/3 responsive genes collagen type 1, connective tissue growth factor, and alpha skeletal actin (*Figure 7D–F*). However, treatment of cells with SRT1720 in the presence of TGF-β1 significantly reduced this effect, demonstrating that SRT1720 attenuates TGF-β signalling and directly affects the downstream fibrotic response.

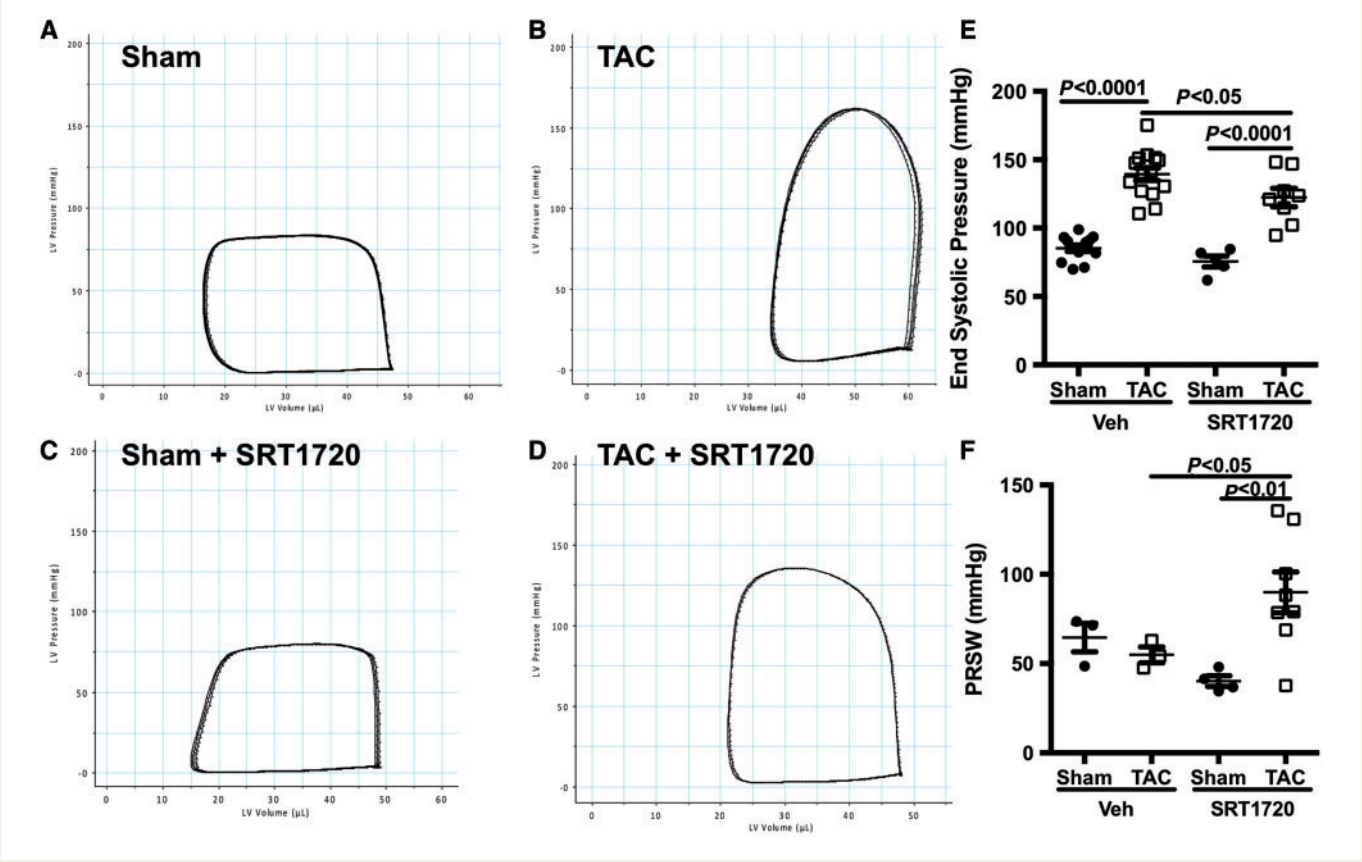

Figure 3 SRT1720 improves cardiac contractility in pressure overload mice. (*A–D*) Steady-state representative PV loops of cardiac function. (*E*) End-systolic pressure was improved with SRT1720 treatment ($n = 5–14$ animals per group); data are presented as mean ± SEM and analysed using a two-way ANOVA with Tukey's *post hoc* test. (*F*) The load insensitive marker of cardiac contractility, the preload recruitable stroke work index was similar in TAC mice compared with sham-operated animals, but was increased in SRT1720-treated TAC mice ($n = 3–8$ animals per group); data are presented as mean ± SEM and analysed using a two-way ANOVA with Tukey's *post hoc* test.

Table 3 Pressure–volume loop data

	Sham ($n = 14$)	Sham + SRT1720 ($n = 5$)	TAC ($n = 14$)	TAC + SRT1720 ($n = 8$)
*P*ed (mmHg)	6.97 ± 1.1	3.62 ± 0.8	9.01 ± 1.8	6.87 ± 1.1
*P*es (mmHg)	85.26 ± 2.3	75.53 ± 4.0	139 ± 4.6*	122 ± 6.7**
Tau (ms)	8.66 ± 0.5	8.33 ± 0.9	7.85 ± 0.7	7.93 ± 0.3
dP/dt max (mmHg/s)	6475 ± 411	6914 ± 958	8497 ± 478*	7328 ± 368
dP/dt min (mmHg/s)	-5771 ± 309	-4848 ± 527	-8090 ± 574*	-6839 ± 405
EDPVR	0.26 ± 0.04	0.19 ± 0.09	0.26 ± 0.09	0.26 ± 0.03
ESPVR	2.82 ± 0.4	2.39 ± 1.0	2.14 ± 0.29	2.85 ± 0.4
PRSW	61.26 ± 4.7	40.20 ± 3.0	56.90 ± 4.7	89 ± 11**

Data are presented as mean ± SEM. All measurements are of the left ventricle.
dP/dt max, maximal rate of pressure rise in the left ventricle; dP/dt min, minimum rate of pressure rise in the left ventricle; EDPVR, end diastolic pressurevolume relationship; ESPVR, end-systolic pressurevolume relationship; Ped, end diastolic pressure; Pes, end-systolic pressure; PRSW, preload recruitable stroke work; TAC, transverse aortic constriction.
*$P < 0.05$ compared with sham using a two-way ANOVA with Tukey's *post hoc* test.
**$P < 0.05$ compared with TAC using a two-way ANOVA with Tukey's *post hoc* test.

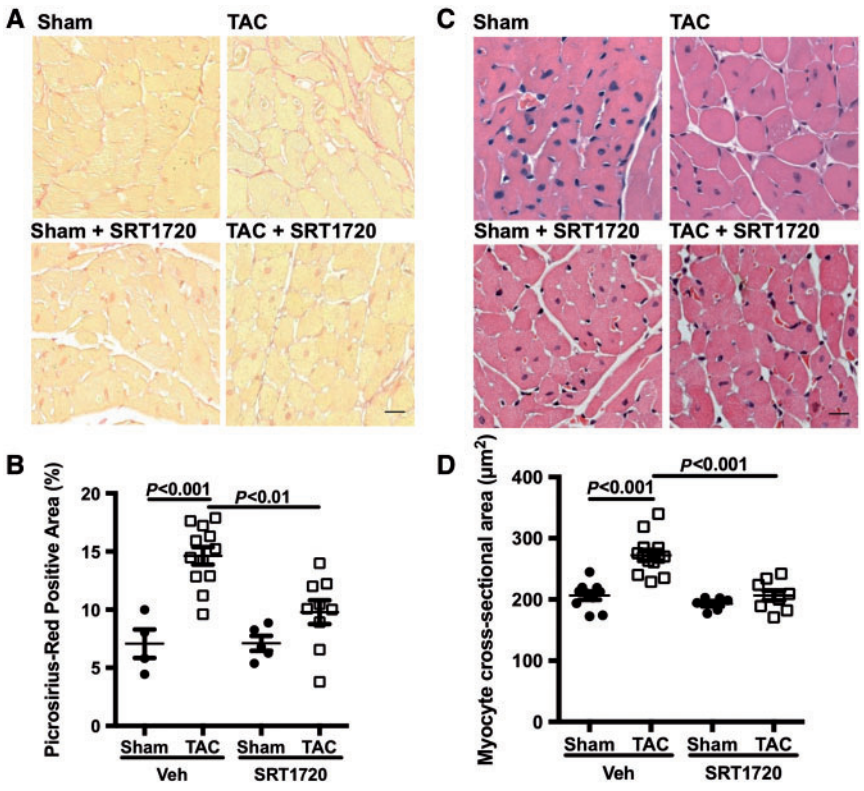

Figure 4 SRT1720 reduces pressure overload-induced cardiac hypertrophy and fibrosis. Representative images of the sub-endocardial zone of LV sections stained with PSR. (*A*) Increased collagen staining observed in TAC-operated animals compared with sham controls was reduced with SRT1720 treatment. (*B*) Quantification of PSR staining intensity ($n = 5$–13 animals per group); data are presented as mean ± SEM and analysed using a two-way ANOVA with Tukey's *post hoc* test. (*C*) The sub-endocardial zone of LV sections stained with haematoxylin and eosin revealed an increase in myocyte size in TAC-operated animals, which was normalized with SRT1720 treatment. (*D*) Quantitative data ($n = 6$–13 animals per group) are presented as mean ± SEM. Scale bar: 20 μm.

Table 4 Foetal gene programme

	Sham ($n = 10$)	Sham + SRT1720 ($n = 6$)	TAC ($n = 6$)	TAC + SRT1720 ($n = 9$)
β-MHC	1.14 ± 0.2	0.50 ± 0.1*	2.02 ± 0.3*	0.34 ± 0.1***
α-MHC	1.03 ± 0.1	0.35 ± 0.1*	0.51 ± 0.1*	0.47 ± 0.1*
β:α-MHC ratio	1.10 ± 0.2	1.45 ± 0.2	3.69 ± 0.7*	0.89 ± 0.2**
SERCA2	1.06 ± 0.1	0.28 ± 0.1*	0.51 ± 0.1*	0.52 ± 0.1*
SKA	1.06 ± 0.1	0.33 ± 0.1	2.63 ± 0.9*	0.75 ± 0.1***
ANP	1.03 ± 0.1	0.53 ± 0.1	3.95 ± 1.7*	0.51 ± 0.01***

Data are presented as mean ± SEM. All values are compared with RPL13a_2 control gene expression.
ANP, atrial natriuretic peptide; MHC, myosin heavy chain; SERCA2, sarcoplasmic reticulum calcium ATPase 2; SKA, skeletal α-actin.
*$P < 0.05$ compared with sham using a two-way ANOVA with Tukey's *post hoc* test
**$P < 0.05$ compared with TAC using a two-way ANOVA with Tukey's *post hoc* test.

4. Discussion

HF is a chronic condition characterized by ventricular remodelling which occurs secondary to a variety of processes including metabolic dysregulation and changes in cardiac gene expression.[26] The various mechanisms responsible for these changes are the subject of intense investigation.[27] Whilst many signalling pathways become dysregulated in the pathogenesis of HF, altered TGF-β signalling has been implicated in both the pathogenesis and progression of HF.[6,28] Although the regulation of canonical TGF-β signalling is complex, the recognition that Smads, downstream mediators of TGF-β activation, require the acetylation of specific lysine residues in the MH1 domain provides a point whereby protein function can be precisely regulated.[29,30] With lysine acetylation via the histone acetyltransferase p300/CBP garnering much interest, the opposing effect of lysine de-acetylase in modifying protein function has also become a focus of investigation.[31,32]

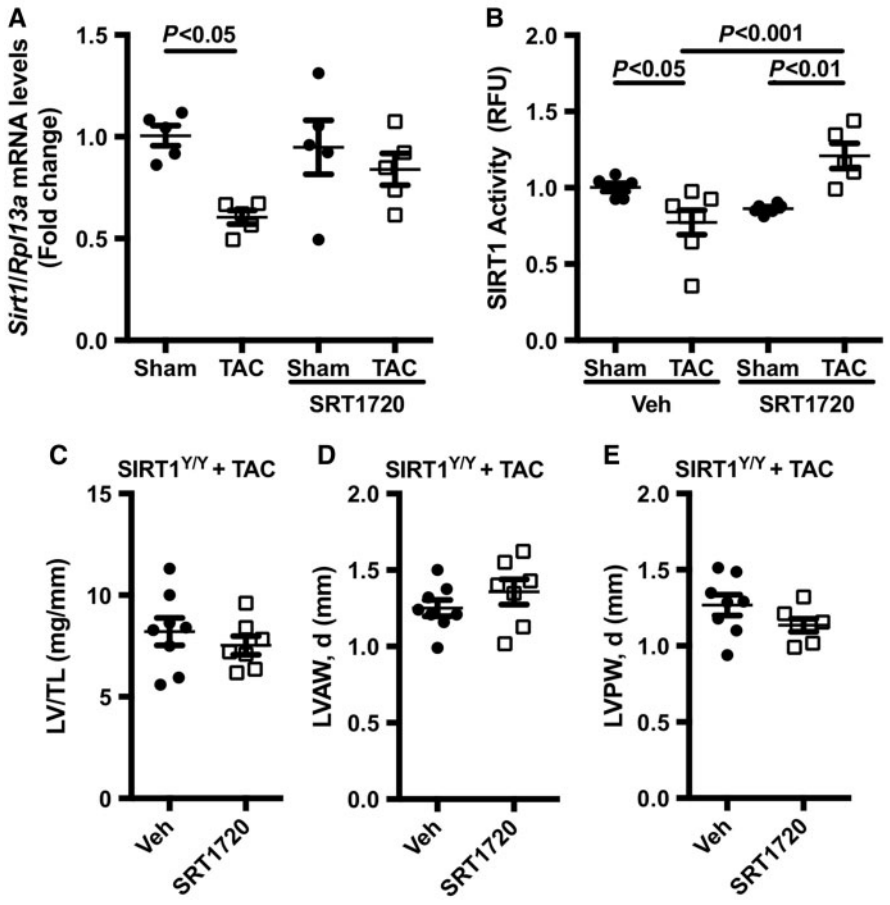

Figure 5 SRT1720 increases SIRT1 de-acetylase activity in pressure overload animals: (*A*) SIRT1 expression ($n = 5$ animals per group) and (*B*) de-acetylase activity ($n = 5$–7 animals per group) were markedly reduced in TAC-operated animals, but normalized with SRT1720 treatment. Data are presented as mean ± SEM and analysed using a two-way ANOVA with Tukey's *post hoc* test. The specificity of SRT1720 was assessed using a SIRT1 catalytically inactive mouse model ($SIRT1^{Y/Y}$). No significant differences in cardiac structure and function were observed in TAC-operated SIRT1Y/Y animals treated with SRT1720 or vehicle. (*C*) Left ventricular (LV) weight normalized to tibia length ($n = 6$–8 animals per group), (*D*) LV anterior wall diameter (LVAW, d; $n = 7$–8 animals per group), and (*E*) LV posterior wall diameter (LVPW, d; $n = 7$–8 animals per group) were not improved with SRT1720 treatment. Data are presented as mean ± SEM and analysed using a two-tailed, unpaired Student's *t*-test.

SIRT1, an enzyme with de-acetylase activity, is a potential candidate that may contribute to the remodelling response.[14] Recent data have emerged demonstrating that sirtuins are involved in key intracellular processes and that substrates of sirtuins include proteins that modulate chromatin folding, metabolic regulation, and stress responses—all of which are dysregulated in HF.[33] In this study, we show that in humans and experimental HF samples, SIRT1 expression and activity are reduced. By increasing the de-acetylase activity of SIRT1 using the compound SRT1720, we were able to prevent ventricular remodelling and reduce TGF-β activation in a murine model of pressure overload. These findings suggest that a loss of SIRT1 de-acetylase activity contributes to ventricular remodelling and that the enhancement of SIRT1 de-acetylase activity, with the use of SRT1720, may be a novel therapeutic target for HF.

At present, there are seven known mammalian sirtuins, with SIRT1 being the best studied in the cardiac literature. The main body of knowledge regarding SIRT1 in cardiac (patho)physiology involves overexpression studies in transgenic mice on a C57BL/6j background. Intriguingly, conflicting results have emerged. Overexpression by approximately nine-fold promotes LV hypertrophy,[34] whereas modest overexpression by approximately three-fold demonstrates a protective and antioxidant effect and reduces ischaemia reperfusion injury.[33] Whilst these studies give insight into the role of SIRT1, they are less clinically relevant.

In this study, we hypothesized that loss of SIRT1 expression and activity may influence gene and protein function directly through a loss of its de-acetylase activity. Of relevance to the current study is TGF-β1, a profibrotic cytokine implicated in the remodelling response and one of the first targets to be identified as modifiable by lysine acetylation.[12] Indeed, our group has shown that inhibition of p300-mediated lysine acetylation of Smad2 reduces TGF-β1 activity both *in vivo* and *in vitro* and prevents the progression to HF in the setting of diabetic cardiomyopathy.[30] As a result, we hypothesize that a loss of SIRT1 de-acetylase activity promotes unopposed Smad2/3 acetylation, thereby augmenting TGF-β1 activity.

Utilizing a well-described murine model of pressure overload, in which TGF-β activity is increased, treatment with SRT1720 significantly inhibited

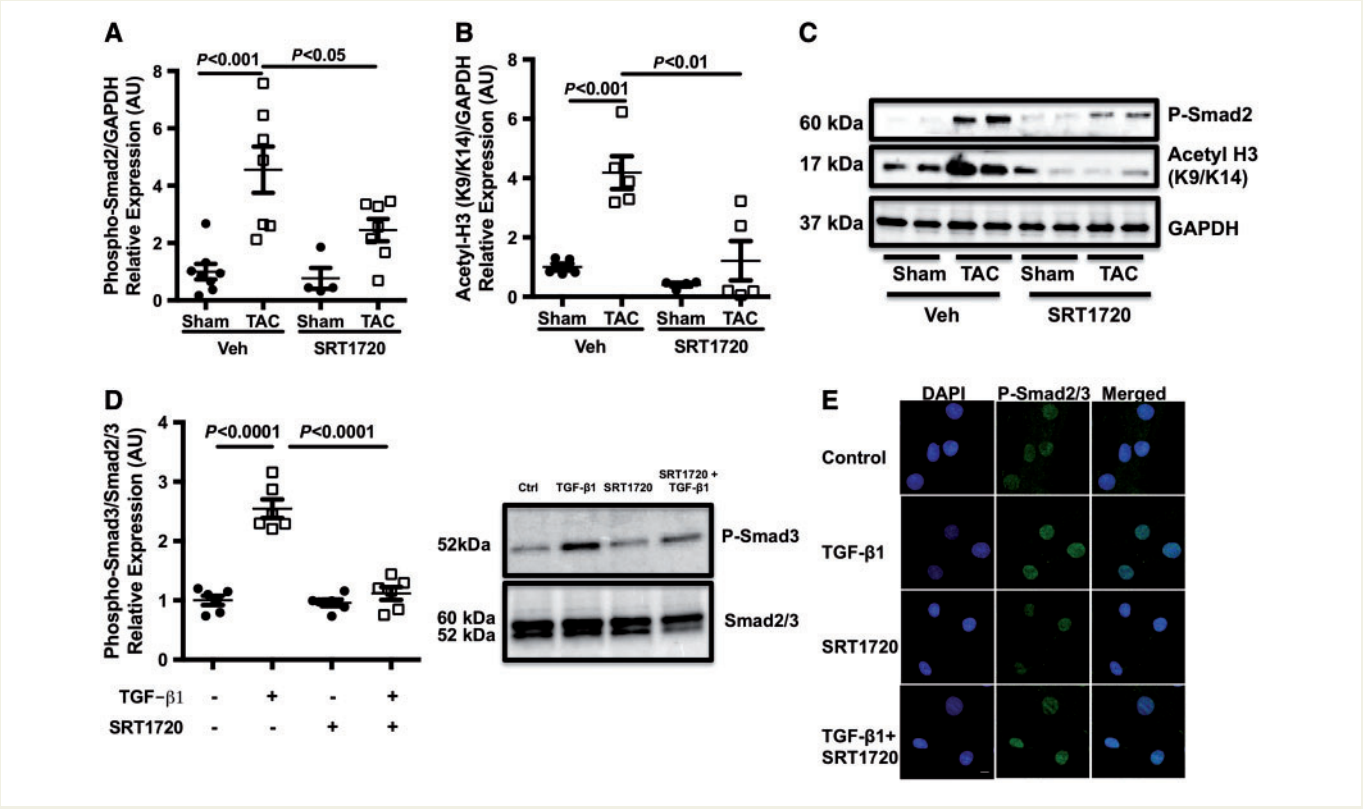

Figure 6 SRT1720 attenuates canonical TGF-β1 signalling: TGF-β1 activity was assessed by quantifying Smad2/3 phosphorylation and acetylation. (*A* and *C*) TAC-induced Smad2 phosphorylation ($n = 6$–8 animals per group) was reduced by treatment with SRT1720. (*B* and *C*) SRT1720 also reduced acetylated histone H3K9/K14 protein expression ($n = 5$ animals per group) in TAC animals compared with their untreated counterparts. Data are presented as mean ± SEM and analysed with two-way ANOVA with Tukey's *post hoc* test. (*D*) Treatment of human cardiac fibroblast cells with TGF-β1 increased Smad3 phosphorylation, which was reduced with SRT1720 treatment ($n = 6$ per group); data are presented as mean ± SEM and analysed with two-way ANOVA with Tukey's *post hoc* test. (*E*) This was corroborated with immunofluorescence microscopy, which revealed an increase in phosphorylated Smad2/3 nuclear localization with TGF-β1 treatment but a reduction with SRT1720 co-treatment ($n = 6$ per group); scale bar: 10 μm.

TGF-β activation and reduced cardiac fibrosis and hypertrophy. The observed reduction in Smad2 phosphorylation, noted with SRT1720 treatment, is consistent with a reduction in canonical TGF-β signalling via inhibition of the well-described TGF-β1 auto-induction loop.[10,35] However, the SRT1720-mediated increase of SIRT1 activity and subsequent diminution of TGF-β signalling and expression of pro-fibrotic genes did not appear to favour Smad2 over Smad3 and *vice versa*. Although Smad3 has been extensively studied and recognized as a key mediator of TGF-β-induced pro-fibrotic outcomes, both Smad2 and Smad3 have been implicated in ECM production and tissue fibrosis.[30,36–38] Indeed, a recent study by Jeffrey Molkentin's group demonstrates that, although Smad2 and Smad3 may play distinct roles in tissue fibrosis, both Smad2 and Smad3 are critical in the induction and maintenance of activated fibroblast activity and fibrosis in the heart, whether in response to pressure overload or TGF-β1 ligand itself.[38] These findings closely align with our observation that SIRT1 activation improves cardiac fibrosis by targeting both Smad2 and Smad3 signalling, as evidenced by reduced Smad2/3 phosphorylation, nuclear translocation, and promoter activity.

Whilst increasing SIRT1 activity improved cardiac function and reduced TGF-β activity, it is likely that other targets are influenced by this approach. SIRT1 has been demonstrated to interact with a variety of other important LV signalling targets such as IGF1, FOXO1, AKT, PGC1-alpha, and the MAP kinases.[39–42] Indeed, de-acetylation of FOXO1 by SIRT1 has been shown to stimulate FOXO1-mediated transcription of anti-oxidants in order to suppress oxidative stress in cardiac myocytes and to protect the heart from ischaemia/reperfusion injury.[33] SIRT1 has also been shown to de-acetylate AKT to modulate its activity and involvement in cellular processes implicated in the development of cardiac hypertrophy and ageing.[43] It can also de-acetylate p53 and attenuate its ability to activate downstream target genes such as p21 and Bax to regulate cell cycle arrest and apoptosis, respectively.[44,45] Whilst this lack of SIRT1 specificity may be perceived as a limitation, in terms of understanding pharmacological mechanism of action, from a translational perspective this may be highly beneficial. For instance, current HF therapies effect many thousands of downstream LV signalling targets, with inhibitors of the angiotensin-converting enzyme cascade being a classic example.[46] Also, novel approaches to the treatment of HF, using microRNA strategies for example, interact with as many as 60–80 genes[47]; therefore, given the complexity of the remodelling response, it is likely that this lack of specificity may in fact be highly beneficial in the *in vivo* setting. Our data demonstrate that the intracellular signalling molecules Smad2/3 are a target of SIRT1 de-acetylase activity and that pharmacological manipulation of SIRT1 activity with the compound SRT1720 results in modification of downstream TGF-β signalling.

To ensure that the functional effects of SRT1720 are not dependent upon altered loading conditions, two complementary state of

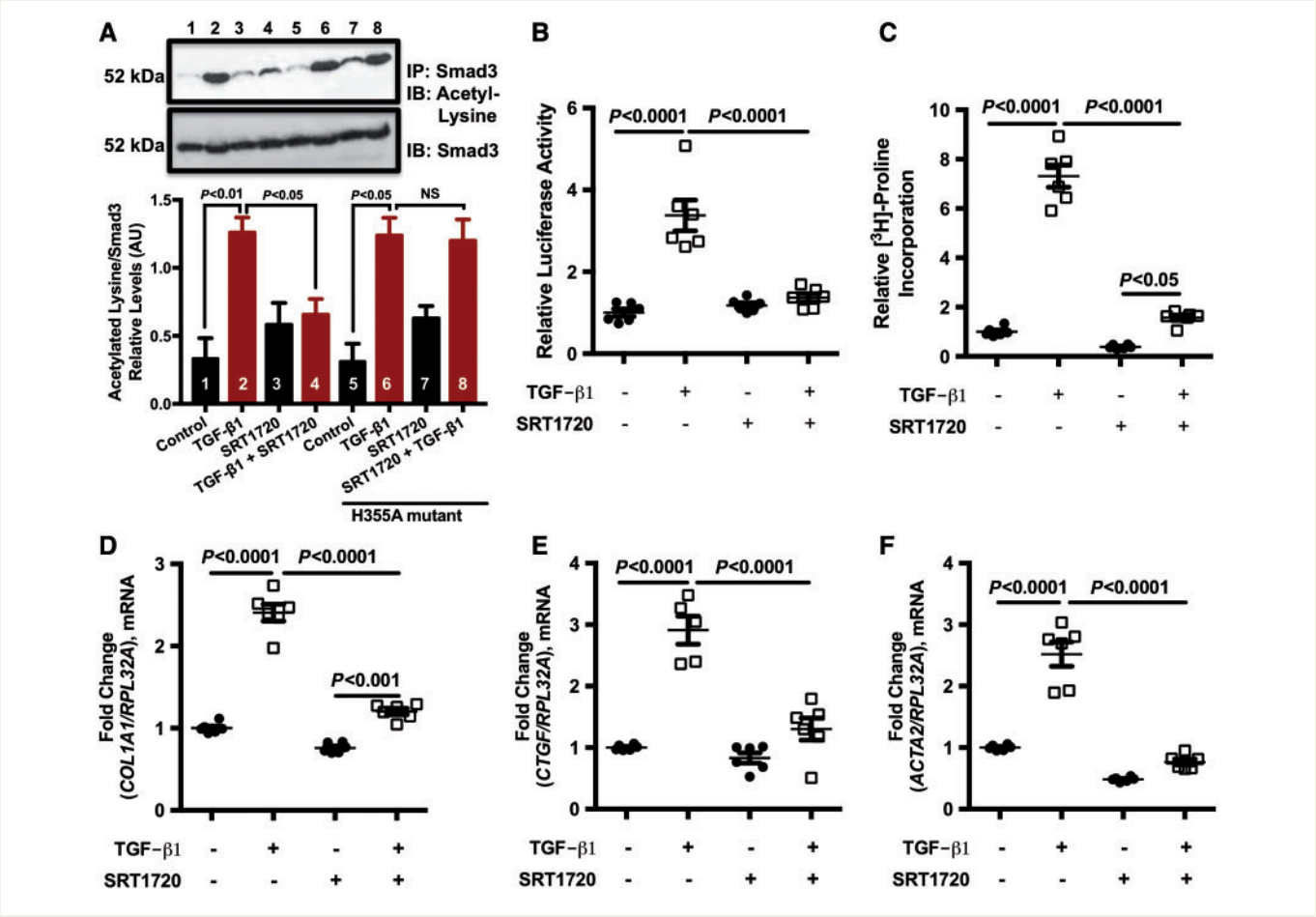

Figure 7 SRT1720 modulates TGF-β fibrotic response. (*A*) Nuclear protein extracted from HEK cells transfected with a SIRT1 catalytically inactive dominant negative mutant (H355A) and stimulated with TGF-β1 in the presence and absence of SRT1720 was isolated. Smad3 acetylation levels were increased with TGF-β1 stimulation both in the absence and in the presence of the dominant negative mutant. This, however, was reduced when cells were pre-treated with SRT1720, in the absence of the dominant negative mutant. The SRT1720-mediated decrease in Smad3 acetylation was abrogated in the presence of H355A mutant. A representative western blot is shown above and quantification data ($n = 5$ per group) presented as mean ± SEM and analysed with two-way ANOVA with Tukey's *post hoc* test. (*B*) HEK cells were transfected with the Smad2/3 reporter construct SBE4-Luc were strongly stimulated by TGF-β1, as assessed by luciferase activity. This, however, was attenuated by SRT1720 ($n = 6$ per group); data are presented as mean ± SEM and analysed with two-way ANOVA with Tukey's *post hoc* test. (*C*) SRT1720 also reduced tritiated proline incorporation ($n = 6$ per group), a marker of collagen synthesis, in cardiac fibroblasts stimulated with TGF-β1 and also reduced the expression of TGF-β responsive genes (*D*) collagen type 1 ($n = 6$ per group), (*E*) connective tissue growth factor ($n = 5$–6 per group), and (*F*) alpha skeletal actin ($n = 6$ per group). Data are presented as mean ± SEM and analysed with two-way ANOVA with Tukey's *post hoc* test.

the art approaches were used to interrogate cardiac function. First, cardiac systolic function was assessed non-invasively using traditional two-dimensional measures of cardiac function such as ejection fraction, complemented with an assessment of regional cardiac function using velocity vector imaging. At 6 weeks post-surgery, global and regional systolic functions were reduced in TAC-operated animals. Despite no significant difference in afterload (as measured by end-systolic pressure), SRT1720 improved global and regional function. These findings were complemented by invasive pressure–volume loop analysis at study termination. Cardiac contractility, as measured by the load-insensitive preload recruitable stroke work index, was improved by treatment with SRT1720. Somewhat surprisingly, there was no difference observed between sham- and TAC-operated animals, in terms of diastolic function. Despite TAC-operated animals demonstrating a marked increase in cardiac fibrosis and hypertrophy, end-diastolic pressure, Tau and the slope of the end-diastolic pressure–volume relationship remained unchanged. These findings are in keeping with that observed by Norton *et al.*[48] in a rat model of pressure overload. Indeed, Klotz *et al.*[49] demonstrated using the Dahl salt-sensitive rat that the slope of the EDPVR may shift upwards, remain unchanged, or shift down and to the right in a time- and geometry-dependent fashion despite overt left ventricular hypertrophy and interstitial fibrosis being present. These results underscore the important distinction between pump dysfunction (which depends not only on muscle function, geometry, LV mass, and activation sequence) and intrinsic myocardial dysfunction, and the need to interrogate cardiac function with multiple, complementary modalities such as echocardiography and invasive PV loops.

In keeping with a significant reduction in LV mass, treatment of TAC-operated animals with SRT1720 inhibited TAC-induced activation of the 'foetal gene programme'. TAC induced β-MHC, SKA, and ANP expression, whilst repressing SERCA 2A and α-MHC expression. SRT1720 in TAC-operated animals normalized the β:α-MHC ratio and reduced ANP expression. Of note, it had no effect on SERCA 2A or α-MHC expression. These findings are different from those observed by Sulaiman *et al.*[50] and Pillai *et al.*[51] who demonstrate that resveratrol, a putative SIRT1 activator, increased both SERCA 2A and α-MHC. Whilst much early excitement was generated by the use of the SIRT1 activator resveratrol[16,52] in the treatment of CV and neurological disease, recent data have tempered such enthusiasm with studies clearly demonstrating the non-specific nature of resveratrol's activity,[53] thus making interpretation of the results difficult. It has not escaped our attention that treatment of sham-operated animals with SRT1720 was accompanied by a reduction in the expression of β-MHC, SERCA 2A, SKA, and ANP, when compared with their untreated counterparts. However, this observation is in keeping with the reported role of SIRT1 as a facilitator of heterochromatin formation and thus general transcriptional repression.[15,54–56] Although SRT1720 altered the expression of the foetal gene programme in sham-operated animals, these changes did not impact cardiac structure and function. Indeed, the hearts of sham-operated animals treated with SRT1720 were structurally and functionally similar to those of untreated sham-operated animals as assessed by echocardiography and cardiac catheterization.

In this study, we utilized SRT1720, a small molecule that was initially shown to increase SIRT1 de-acetylase activity up to 781% at orders of magnitude lower concentrations than resveratrol.[18] However, more recently the specificity of SIRT1 activating compounds (STACs) such as SRT1720 has been questioned.[53] To address this, we utilized multiple different methods, including a genetically modified SIRT1 inactive model and cells transfected with a SIRT1 catalytically inactive mutant (H355A) to demonstrate specificity. Our data demonstrate that SRT1720 reduces Smad acetylation *in vitro* and that this effect was lost when SIRT1 was modified to a catalytically inactive mutant form. Furthermore, work by our group has demonstrated that another STAC, SRT3025, improved both renal and cardiac structure and function in a rodent model of progressive kidney disease.[57] However, it should be noted that while the precise sub-molecular target that accounts for an increase in SIRT1 de-acetylase activity by SRT1720 is incompletely understood, recent data suggest it activates SIRT1-mediated de-acetylation via an allosteric mechanism.[18,58] These findings are in keeping with the initial studies by Milne *et al.*[18] and demonstrate the specificity of STAC's for SIRT1 activation and their potential beneficial role in cardiovascular disease.[59]

5. Conclusion

Despite significant therapeutic advances, the mortality and morbidity of HF remains high, and it is one of the health care systems most expensive diagnosis, Our data demonstrate that pharmacological activation of SIRT1 using the compound SRT1720 prevents remodelling in pressure overload mice and that the intracellular signalling molecule Smad2/3 is a likely target of the SRT1720-mediated increase in SIRT1 de-acetylase activity. Altogether, these findings suggest that enhancing SIRT1 activity may be a novel therapeutic strategy to prevent/reverse HF.

Supplementary material

Supplementary material is available at *Cardiovascular Research* online.

Acknowledgements

The authors would like to thank Mr. Mark Gordon at the Keenan Research Centre for Biomedical Science, St. Michael's Hospital for his assistance with Western blotting.

Conflict of interest: none declared.

Funding

This work was supported by a grant from the Heart and Stroke Foundation of Canada [#NA6201 to K.A.C.]. K.A.C. is also a recipient of a New Investigator Award from the Canadian Institutes of Health Research and an Early Researcher Award from the Ministry of Ontario. A Canadian Institutes of Health Research Operating Grant [FRN119368 to R.E.G.] also supported this work. R.E.G. is a Canada Research Chair in Diabetes, and this work was supported in part by the Canada Research Chairs.

References

1. Yeung DF, Boom NK, Guo H, Lee DS, Schultz SE, Tu JV. Trends in the incidence and outcomes of heart failure in Ontario, Canada: 1997 to 2007. *CMAJ* 2012;**184**:E765–E773.
2. Talior-Volodarsky I, Connelly KA, Arora PD, Gullberg D, McCulloch CA. α11 integrin stimulates myofibroblast differentiation in diabetic cardiomyopathy. *Cardiovasc Res* 2012;**96**:265–275.
3. Connelly KA, Kelly DJ, Zhang Y, Prior DL, Martin J, Cox AJ, Thai K, Feneley MP, Tsoporis J, White KE, Krum H, Gilbert RE. Functional, structural and molecular aspects of diastolic heart failure in the diabetic (mRen-2)27 rat. *Cardiovasc Res* 2007;**76**:280–291.
4. Connelly KA, Kelly DJ, Zhang Y, Prior DL, Advani A, Cox AJ, Thai K, Krum H, Gilbert RE. Inhibition of protein kinase C-beta by ruboxistaurin preserves cardiac function and reduces extracellular matrix production in diabetic cardiomyopathy. *Circ Heart Fail* 2009;**2**:129–137.
5. Yuen DA, Connelly KA, Advani A, Liao C, Kuliszewski MA, Trogadis J, Thai K, Advani SL, Zhang Y, Kelly DJ, Leong-Poi H, Keating A, Marsden PA, Stewart DJ, Gilbert RE. Culture-modified bone marrow cells attenuate cardiac and renal injury in a chronic kidney disease rat model via a novel antifibrotic mechanism. *PLoS One* 2010;**5**:e9543.
6. Hein S, Arnon E, Kostin S, Schonburg M, Elsasser A, Polyakova V, Bauer EP, Klovekorn WP, Schaper J. Progression from compensated hypertrophy to failure in the pressure-overloaded human heart: structural deterioration and compensatory mechanisms. *Circulation* 2003;**107**:984–991.
7. Asbun J, Villarreal FJ. The pathogenesis of myocardial fibrosis in the setting of diabetic cardiomyopathy. *J Am Coll Cardiol* 2006;**47**:693–700.
8. Leask A, Abraham DJ. TGF-beta signaling and the fibrotic response. *FASEB J* 2004;**18**:816–827.
9. Border WA, Noble NA. Fibrosis linked to TGF-beta in yet another disease. *J Clin Invest* 1995;**96**:655–656.
10. Rosenkranz S. TGF-beta1 and angiotensin networking in cardiac remodeling. *Cardiovasc Res* 2004;**63**:423–432.
11. Choudhary C, Kumar C, Gnad F, Nielsen ML, Rehman M, Walther TC, Olsen JV, Mann M. Lysine acetylation targets protein complexes and co-regulates major cellular functions. *Science* 2009;**325**:834–840.
12. Simonsson M, Kanduri M, Gronroos E, Heldin CH, Ericsson J. The DNA binding activities of Smad2 and Smad3 are regulated by coactivator-mediated acetylation. *J Biol Chem* 2006;**281**:39870–39880.
13. Ross S, Cheung E, Petrakis TG, Howell M, Kraus WL, Hill CS. Smads orchestrate specific histone modifications and chromatin remodeling to activate transcription. *EMBO J* 2006;**25**:4490–4502.
14. Guarente L. Franklin H. Epstein Lecture: sirtuins, aging, and medicine. *N Engl J Med* 2011;**364**:2235–2244.
15. Imai S, Armstrong CM, Kaeberlein M, Guarente L. Transcriptional silencing and longevity protein Sir2 is an NAD-dependent histone deacetylase. *Nature* 2000;**403**:795–800.
16. Lagouge M, Argmann C, Gerhart-Hines Z, Meziane H, Lerin C, Daussin F, Messadeq N, Milne J, Lambert P, Elliott P, Geny B, Laakso M, Puigserver P, Auwerx J. Resveratrol improves mitochondrial function and protects against metabolic disease by activating SIRT1 and PGC-1alpha. *Cell* 2006;**127**:1109–1122.

17. Bindu S, Pillai VB, Gupta MP. Role of sirtuins in regulating pathophysiology of the heart. *Trends Endocrinol Metab* 2016;**27**:563–573.
18. Milne JC, Lambert PD, Schenk S, Carney DP, Smith JJ, Gagne DJ, Jin L, Boss O, Perni RB, Vu CB, Bemis JE, Xie R, Disch JS, Ng PY, Nunes JJ, Lynch AV, Yang H, Galonek H, Israelian K, Choy W, Iffland A, Lavu S, Medvedik O, Sinclair DA, Olefsky JM, Jirousek MR, Elliott PJ, Westphal CH. Small molecule activators of SIRT1 as therapeutics for the treatment of type 2 diabetes. *Nature* 2007;**450**:712–716.
19. Papp S, Dziak E, Kabir G, Backx P, Clement S, Opas M. Evidence for calreticulin attenuation of cardiac hypertrophy induced by pressure overload and soluble agonists. *Am J Pathol* 2010;**176**:1113–1121.
20. Seifert EL, Caron AZ, Morin K, Coulombe J, He XH, Jardine K, Dewar-Darch D, Boekelheide K, Harper ME, McBurney MW. SirT1 catalytic activity is required for male fertility and metabolic homeostasis in mice. *FASEB J* 2012;**26**:555–566.
21. Tsui AK, Marsden PA, Mazer CD, Adamson SL, Henkelman RM, Ho JJ, Wilson DF, Heximer SP, Connelly KA, Bolz SS, Lidington D, El-Beheiry MH, Dattani ND, Chen KM, Hare GM. Priming of hypoxia-inducible factor by neuronal nitric oxide synthase is essential for adaptive responses to severe anemia. *Proc Natl Acad Sci USA* 2011;**108**:17544–17549.
22. Chong A, Maclaren G, Chen R, Connelly KA. Perioperative applications of deformation (myocardial strain) imaging with speckle-tracking echocardiography. *J Cardiothorac Vasc Anesth* 2014;**28**:128–140.
23. Kelly DJ, Zhang Y, Connelly K, Cox AJ, Martin J, Krum H, Gilbert RE. Tranilast attenuates diastolic dysfunction and structural injury in experimental diabetic cardiomyopathy. *Am J Physiol Heart Circ Physiol* 2007;**293**:H2860–H2869.
24. Connelly KA, Advani A, Kim S, Advani SL, Zhang M, White KE, Kim YM, Parker C, Thai K, Krum H, Kelly DJ, Gilbert RE. The cardiac (pro)renin receptor is primarily expressed in myocyte transverse tubules and is increased in experimental diabetic cardiomyopathy. *J Hypertens* 2011;**29**:1175–1184.
25. Advani A, Kelly DJ, Cox AJ, White KE, Advani SL, Thai K, Connelly KA, Yuen D, Trogadis J, Herzenberg AM, Kuliszewski MA, Leong-Poi H, Gilbert RE. The (Pro)renin receptor: site-specific and functional linkage to the vacuolar H+-ATPase in the kidney. *Hypertension* 2009;**54**:261–269.
26. Xie M, Burchfield JS, Hill JA. Pathological ventricular remodeling: therapies: part 2 of 2. *Circulation* 2013;**128**:1021–1030.
27. Kehat I, Molkentin JD. Molecular pathways underlying cardiac remodeling during pathophysiological stimulation. *Circulation* 2010;**122**:2727–2735.
28. Border WA, Noble NA. Transforming growth factor beta in tissue fibrosis. *N Engl J Med* 1994;**331**:1286–1292.
29. Inoue Y, Itoh Y, Abe K, Okamoto T, Daitoku H, Fukamizu A, Onozaki K, Hayashi H. Smad3 is acetylated by p300/CBP to regulate its transactivation activity. *Oncogene* 2007;**26**:500–508.
30. Bugyei-Twum A, Advani A, Advani SL, Zhang Y, Thai K, Kelly DJ, Connelly KA. High glucose induces Smad activation via the transcriptional coregulator p300 and contributes to cardiac fibrosis and hypertrophy. *Cardiovasc Diabetol* 2014;**13**:89.
31. Advani A, Huang Q, Thai K, Advani SL, White KE, Kelly DJ, Yuen DA, Connelly KA, Marsden PA, Gilbert RE. Long-term administration of the histone deacetylase inhibitor vorinostat attenuates renal injury in experimental diabetes through an endothelial nitric oxide synthase-dependent mechanism. *Am J Pathol* 2011;**178**:2205–2214.
32. Bush EW, McKinsey TA. Protein acetylation in the cardiorenal axis: the promise of histone deacetylase inhibitors. *Circ Res* 2010;**106**:272–284.
33. Hsu CP, Zhai P, Yamamoto T, Maejima Y, Matsushima S, Hariharan N, Shao D, Takagi H, Oka S, Sadoshima J. Silent information regulator 1 protects the heart from ischemia/reperfusion. *Circulation* 2010;**122**:2170–2182.
34. Alcendor RR, Gao S, Zhai P, Zablocki D, Holle E, Yu X, Tian B, Wagner T, Vatner SF, Sadoshima J. Sirt1 regulates aging and resistance to oxidative stress in the heart. *Circ Res* 2007;**100**:1512–1521.
35. Van Obberghen-Schilling E, Thompson N, Flanders K, Sporn M, Lambert P, Baker C. Transforming growth factor beta 1 positively regulates its own expression in normal and transformed cells. *J Biol Chem* 1988;**263**:7741–7746.
36. Bujak M, Ren G, Kweon HJ, Dobaczewski M, Reddy A, Taffet G, Wang XF, Frangogiannis NG. Essential role of Smad3 in infarct healing and in the pathogenesis of cardiac remodeling. *Circulation* 2007;**116**:2127–2138.
37. Zhao J, Shi W, Wang YL, Chen H, Bringas P Jr, Datto MB, Frederick JP, Wang XF, Warburton D. Smad3 deficiency attenuates bleomycin-induced pulmonary fibrosis in mice. *Am J Physiol Lung Cell Mol Physiol* 2002;**282**:L585–L593.
38. Khalil H, Kanisicak O, Prasad V, Correll RN, Fu X, Schips T, Vagnozzi RJ, Liu R, Huynh T, Lee SJ, Karch J, Molkentin JD. Fibroblast-specific TGF-beta-Smad2/3 signaling underlies cardiac fibrosis. *J Clin Invest* 2017;**127**:3770–3783.
39. Vahtola E, Louhelainen M, Forsten H, Merasto S, Raivio J, Kaheinen P, Kyto V, Tikkanen I, Levijoki J, Mervaala E. Sirtuin1-p53, forkhead box O3a, p38 and post-infarct cardiac remodeling in the spontaneously diabetic Goto-Kakizaki rat. *Cardiovasc Diabetol* 2010;**9**:5.
40. Rahman S, Islam R. Mammalian Sirt1: insights on its biological functions. *Cell Commun Signal* 2011;**9**:11.
41. Feige JN, Lagouge M, Canto C, Strehle A, Houten SM, Milne JC, Lambert PD, Mataki C, Elliott PJ, Auwerx J. Specific SIRT1 activation mimics low energy levels and protects against diet-induced metabolic disorders by enhancing fat oxidation. *Cell Metab* 2008;**8**:347–358.
42. Oka S, Alcendor R, Zhai P, Park JY, Shao D, Cho J, Yamamoto T, Tian B, Sadoshima J. PPARalpha-Sirt1 complex mediates cardiac hypertrophy and failure through suppression of the ERR transcriptional pathway. *Cell Metab* 2011;**14**:598–611.
43. Pillai VB, Sundaresan NR, Gupta MP. Regulation of Akt signaling by sirtuins: its implication in cardiac hypertrophy and aging. *Circ Res* 2014;**114**:368–378.
44. Luo J, Nikolaev AY, Imai S, Chen D, Su F, Shiloh A, Guarente L, Gu W. Negative control of p53 by Sir2alpha promotes cell survival under stress. *Cell* 2001;**107**:137–148.
45. Vaziri H, Dessain SK, Ng Eaton E, Imai SI, Frye RA, Pandita TK, Guarente L, Weinberg RA. hSIR2(SIRT1) functions as an NAD-dependent p53 deacetylase. *Cell* 2001;**107**:149–159.
46. Campos AH, Zhao Y, Pollman MJ, Gibbons GH. DNA microarray profiling to identify angiotensin-responsive genes in vascular smooth muscle cells: potential mediators of vascular disease. *Circ Res* 2003;**92**:111–118.
47. van Rooij E, Olson EN. MicroRNAs: powerful new regulators of heart disease and provocative therapeutic targets. *J Clin Invest* 2007;**117**:2369–2376.
48. Norton GR, Woodiwiss AJ, Gaasch WH, Mela T, Chung ES, Aurigemma GP, Meyer TE. Heart failure in pressure overload hypertrophy. The relative roles of ventricular remodeling and myocardial dysfunction. *J Am Coll Cardiol* 2002;**39**:664–671.
49. Klotz S, Hay I, Zhang G, Maurer M, Wang J, Burkhoff D. Development of heart failure in chronic hypertensive Dahl rats: focus on heart failure with preserved ejection fraction. *Hypertension* 2006;**47**:901–911.
50. Sulaiman M, Matta MJ, Sunderesan NR, Gupta MP, Periasamy M, Gupta M. Resveratrol, an activator of SIRT1, upregulates sarcoplasmic calcium ATPase and improves cardiac function in diabetic cardiomyopathy. *Am J Physiol Heart Circ Physiol* 2010;**298**:H833–H843.
51. Pillai JB, Chen M, Rajamohan SB, Samant S, Pillai VB, Gupta M, Gupta MP. Activation of SIRT1, a class III histone deacetylase, contributes to fructose feeding-mediated induction of the alpha-myosin heavy chain expression. *Am J Physiol Heart Circ Physiol* 2008;**294**:H1388–H1397.
52. Dolinsky VW, Chan AY, Robillard Frayne I, Light PE, Des Rosiers C, Dyck JR. Resveratrol prevents the prohypertrophic effects of oxidative stress on LKB1. *Circulation* 2009;**119**:1643–1652.
53. Pacholec M, Bleasdale JE, Chrunyk B, Cunningham D, Flynn D, Garofalo RS, Griffith D, Griffor M, Loulakis P, Pabst B, Qiu X, Stockman B, Thanabal V, Varghese A, Ward J, Withka J, Ahn K. SRT1720, SRT2183, SRT1460, and resveratrol are not direct activators of SIRT1. *J Biol Chem* 2010;**285**:8340–8351.
54. Zhang T, Kraus WL. SIRT1-dependent regulation of chromatin and transcription: linking NAD(+) metabolism and signaling to the control of cellular functions. *Biochim Biophys Acta* 2010;**1804**:1666–1675.
55. Michan S, Sinclair D. Sirtuins in mammals: insights into their biological function. *Biochem J* 2007;**404**:1–13.
56. Guarente L. Sir2 links chromatin silencing, metabolism, and aging. *Genes Dev* 2000;**14**:1021–1026.
57. Zhang Y, Connelly KA, Thai K, Wu X, Kapus A, Kepecs D, Gilbert RE. Sirtuin 1 activation reduces transforming growth factor-beta1-induced fibrogenesis and affords organ protection in a model of progressive, experimental kidney and associated cardiac disease. *Am J Pathol* 2017;**187**:80–90.
58. Dai H, Kustigian L, Carney D, Case A, Considine T, Hubbard BP, Perni RB, Riera TV, Szczepankiewicz B, Vlasuk GP, Stein RL. SIRT1 activation by small molecules: kinetic and biophysical evidence for direct interaction of enzyme and activator. *J Biol Chem* 2010;**285**:32695–32703.
59. Winnik S, Auwerx J, Sinclair DA, Matter CM. Protective effects of sirtuins in cardiovascular diseases: from bench to bedside. *Eur Heart J* 2015;**36**:3404–3412.